Quarterly

Newsletter– Winter 2020 Issue

doi: 10.25923/ymt5-wz59
Vol. 13 No 4, 2020
Editor: Manik Bali, ESSIC UMD

CMA • CNES • ESA • EUMETSAT • IMD • ISRO • JAA • JMA • KMA • NASA • NIST • NOAA • ROSCOSMOS . ROSHYDROMET • SITP • USGS • WMO

In this Issue

Articles

News in This Quarter

Announcements

GSICS Related Publications

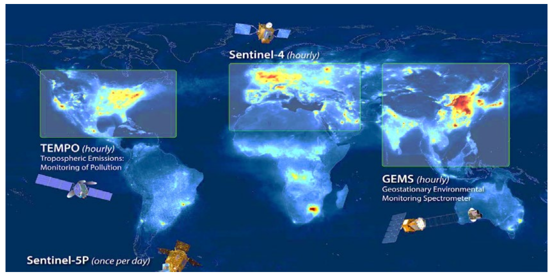

Coverage of GK-2B the first UV GEO compliments S4 and Tempo in UV measurements

Artist rendition of Megha-Tropiques (Image Curtsy EO Portal)

Using ScaRaB on board Megha-Tropiques to investigate the calibration of geostationary thermal infrared channels for cold cloud studies

By Thomas Fiolleau and Rémy Roca
Laboratoire d'Etudes en Géophysique et Océanographie Spatiales/CNRS, Toulouse, France

The characterization of the calibration of the geostationary thermal IR channels is an important step towards a better use of this invaluable resource for operational and scientific applications. Yet the cold part of the IR spectrum (BT<240K) has received relatively less attention than the warmer end (Hewison et al. 2013) limiting its use for cold cloud related studies. It prompted us to perform inter-comparisons using the ScaRaB radiometer on board the Megha-Tropiques mission (Roca et al. 2015) as a baseline for our investigations in the cold BT regime.

The ScaRaB-3 instrument is a broad band radiometer dedicated to the measurements of the Earth radiative budget. Using an elaborate onboard calibration procedure, the instrument is expected to provide highly accurate shortwave and longwave flux estimates within ~1% uncertainty (k=1) (Rosak et al. 2012; Karouche et al. 2012). Such performances have been confirmed thanks to comparisons with the NASA CERES instrument (Trémas et al. 2016). ScaRaB also carries a narrow band thermal IR 10-12 microns channel that also benefits from these demanding performance requirements and is used to evaluate the calibration of the georing thermal IR data.

The inter-comparison study performed over the 2012-2016 period using all available geostationary platforms reveals 10 days' average differences varying from -3K to +3K with respect to ScaRaB (Fiolleau et al., 2020). A statistical method has then been developed to inter-calibrate and to normalize spectrally the geostationary thermal channels to the ScaRaB narrow band reference. The homogenization method relies on collocations between the geostationary observations and the ScaRaB reference.

Assuming that the infrared radiometers on board geostationary platforms have a linear response when observing high cold cloud scenes, the calibration and spectral normalization corrections are based on linear regressions computed every 10 days and over a 10-day period for BT < 240 K. This period of correction is required to prevent high frequency variation of the calibration issues.). Various other aspects of the GEOring homogenization are also included in the study, as well as a limb correction effort. When averaged over the whole period, the final product (after limb correction) mean bias is around 0 K with a standard deviation of less than 1.5K making it suitable for many cold cloud applications. In particular, the homogenized GEO-ring archive is now been used with the TOOCAN algorithm (Fiolleau and Roca 2013) to document the life cycle of tropical convective systems (http://toocan.ipsl.fr).

Contrary to sun-synchronous platforms, Megha-Tropiques has a precessing orbit that allows to sample all the local times every 51 days, offering a unique opportunity to further investigate the IR calibration in cold cloud scenes at the diurnal scale. Figure 1 shows the preliminary results of the diurnal variation of the biases in brightness temperatures for all the homogenized geostationary imagers with respect to the ScaRaB observations in the range [180K-235K]. Note that for this preliminary study, we consider the SEVIRI imager of all the operational MSG platforms over the 5-year period as a single instrument and present multi-MSG averaged results. First, we can observe that all the GEO imagers present a variation of the bias with the local hours. Whatever the GEO platform considered, the minimum BT bias is observed between 20:00 and 04:00, and the maximum is observed for local time between 08:00 and 18:00.

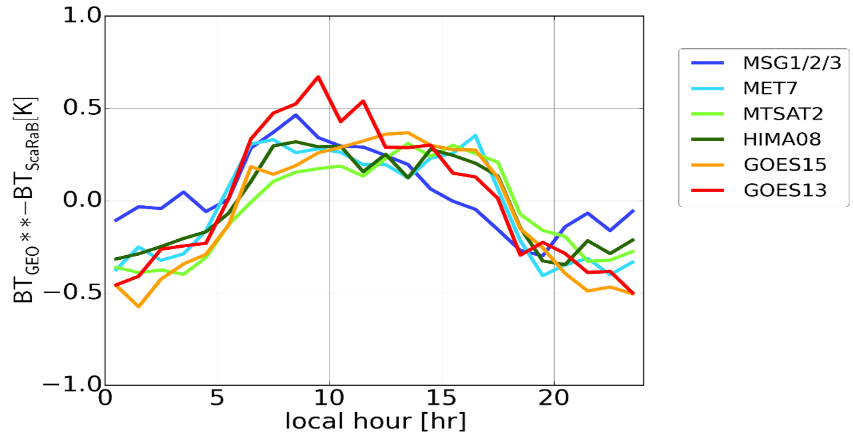

Figure 1: Diurnal variation of the biases in brightness temperature for all the homogenized geostationary thermal infrared channels with respect to the Scarab observations in the range [180K-235K] over the period 2012-2016.

The amplitude of the MSG/SEVIRI then exhibits a relative smaller day/night magnitude around 0.76 K compared to the other GEO platforms. The maximum day/night amplitude is observed for the GOES-13 imager (~ 1.19 K). Note that overall, the day/night magnitude does not exceed 1K for the other GEO platforms. If this result was expected for the 3-axis stabilized geostationary platforms (GOES-13, GOES-15, MTSAT-2, HIMAWARI-8), and is in line with previous analysis (Yu et al. 2013), the spin-stabilized geostationary platforms (MSG, METEOSAT) are expected to be less sensitive to the midnight effects. However, the magnitude of the diurnal variation reported here for the spin-stabilized geostationary platforms is consistent with the results obtained between METEOSAT-9 and VIRS/TRMM (Scarino et al. 2017). This very preliminary investigation of diurnal calibration using ScaRaB on board the precessing Megha-Tropiques satellite completes previous efforts to use hyperspectral instruments and imagers on various platforms to characterize the calibration at diurnal scale. Further work is nevertheless required to attribute the estimated biases to the geostationary instruments or…. to ScaRaB ! comparisons between AIRS, IASI and ScaRaB could contribute to further consolidate these preliminary comparisons.

References:

Fiolleau, T., and R. Roca, 2013: An algorithm for the detection and tracking of tropical mesoscale convective systems using infrared images from geostationary satellite. *IEEE Trans. Geosci. Remote Sens.*, **51**, 4302–4315.

Fiolleau, T., R. Roca, S. Cloché, D. Bouniol, P. Raberanto, 2020: Homogenization of geostationary infrared imager channels for cold cloud studies using Megha-Tropiques/ScaRaB. IEEE Trans. Geosci. Remote Sens., (in revision)

Hewison, T. J., X. Wu, F. Yu, Y. Tahara, X. Hu, D. Kim, and M. Koenig, 2013: GSICS inter-calibration of infrared channels of geostationary imagers using metop/IASI. IEEE Trans. Geosci. Remote Sens., 51, 1160–1170, doi:10.1109/TGRS.2013.2238544.

Karouche, N., C. Goldstein, A. Rosak, C. Malassingne, and G. Raju, 2012: MEGHA-TROPIQUES satellite mission: In flight performances results. *Geoscience and Remote Sensing Symposium*

Return to Page One

doi: 10.25923/ymt5-wz59

(IGARSS), 2012 IEEE International, 4684–4687.

Roca, R., and Coauthors, 2015: The Megha-Tropiques mission: a review after three years in orbit. *Front. Earth Sci.*, **3**, 17.

Rosak, A., T. Tremas, N. Karouche, L. Gillot, and O. Simonella, 2012: Radiometric and geometric scarab-megha-tropiques ground calibration comparison with first in orbit calibration. *Geoscience and Remote Sensing Symposium (IGARSS), 2012 IEEE International*, 4746–4749.

Scarino, B. R., D. R. Doelling, C. O. Haney, K. M. Bedka, P. Minnis, A. Gopalan, and R. Bhatt, 2017: Utilizing the precessing orbit of TRMM to produce hourly corrections of geostationary infrared imager data with the VIRS sensor. *Infrared Remote Sensing and Instrumentation XXV.,Vol 10403,pp 114 -- 127, International Society for Optics and Photonics, https://doi.org/10.1117/12.2273883*

Trémas, T. L., O. Aznay, and O. Chomette, 2016: ScaRaB and CERES-Terra: results of the inter-comparison campaigns. *Infrared Remote Sensing and Instrumentation XXIV*, Vol. 9973 of, 99730B.

Yu, F., X. Wu, M. K. R. V. Raja, Y. Li, L. Wang, and M. Goldberg, 2013: Diurnal and scan angle variations in the calibration of GOES imager infrared channels. *IEEE Trans. Geosci. Remote Sens.*, **51**, 671–683, doi:10.1109/TGRS.2012.2197627.

Discuss the Article

The Copernicus Imaging Microwave Radiometer Mission (CIMR)

By C. Donlon, ESA/ESTEC

Climate change and globalisation are the dominant drivers of societal impacts in the Arctic with rising temperatures and economic development rapidly transforming the physical and biogeochemical environment and the geo-politics of the region. Several areas of extreme concern have been recently raised by the International Panel on climate Change. In response, the European Commission and the High Representative of the Union for Foreign Affairs and Security Policy issued to the European Parliament and the Council, on 27 April 2016, a joint communication that proposed "*An integrated European Union policy for the Arctic*". Continuously monitoring the vast and harsh Arctic environment in a changing world is considered essential to the successful implementation and effective management of the *Arctic Policy*. Copernicus (http://www.copernicus.eu/) is a European system for monitoring the Earth in support of European policy. The system includes space-based infrastructure comprising Earth Observation satellites, ground-based measurement infrastructure, and a set of Copernicus operational services to process these data and provide users with timely, reliable and up-to-date information for the Atmosphere, Marine, Land, Climate Change, Emergency and Security themes. These Services provide critical information to support a wide range of downstream applications. The primary users of Copernicus services are policymakers and public authorities that need information to develop environmental legislation and policies or to, for instance, take critical decisions in the event of an emergency, such as a natural disaster or a humanitarian crisis.

The intense use and increasing awareness of Copernicus has generated great expectations for an evolving Copernicus system. New high-priority requirements from key Arctic user communities have emerged from the European Commission that highlight the need for new satellite measurements that are not currently available from of the existing Copernicus satellite fleet. A number of microwave radiometer missions uniquely observe a wide range of floating sea ice, oceanographic land and atmospheric parameters to serve operational user needs both day and night, and under non-precipitating atmosphere conditions. However, the continuity and operational status of existing missions are not guaranteed. CIMR will fly in a dawn-dusk orbit providing, with one satellite, ~95% global coverage every day (except for rain conditions), better than daily coverage poleward of 55°N and S, and no gap in coverage at the pole itself (Figure 1). CIMR will operate in synergy with the EUMETSAT MetOp-SG(B) mission so that in the polar regions (>65°N and 65°S) collocated and contemporaneous measurements between CIMR and MetOp MWI/ICI and SCA measurements will be available within +/-10 minutes as shown in Figure.2.

Return to Page One

doi: 10.25923/ymt5-wz59
GSICS Quarterly: Winter Issue 2020 Volume 13, No. 4, 2020

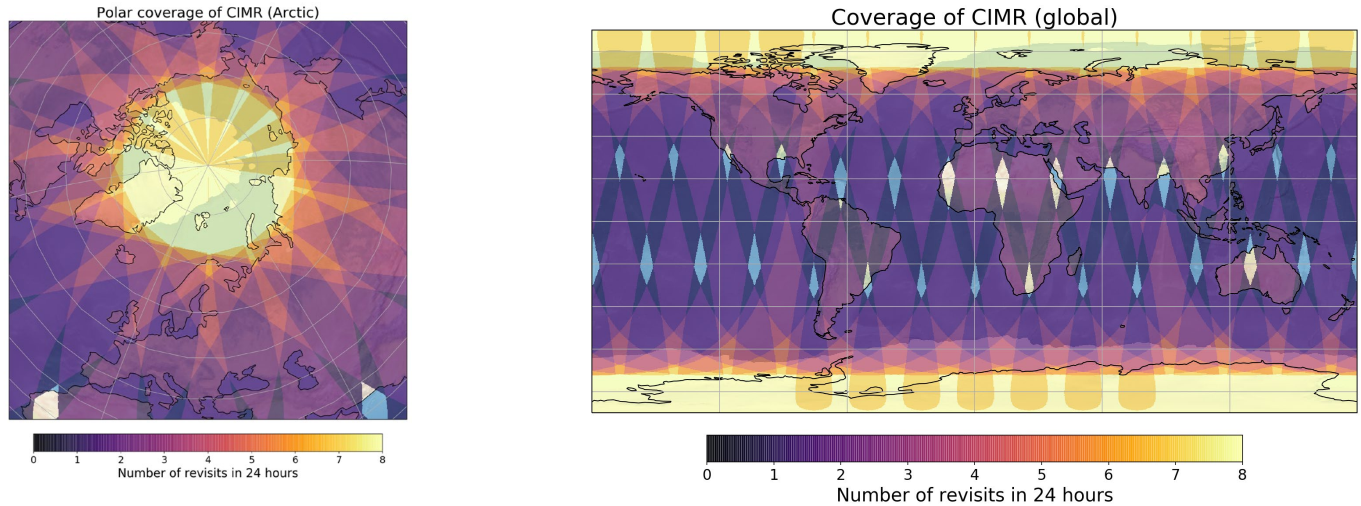

Figure 1. Example maps showing a simulation of the expected CIMR global coverage over the Arctic, using a single satellite, highlighting the number of revisits each day with no hole at the pole. Daily coverage of the Copernicus Imaging Microwave Radiometer mission in the Arctic regions. The colormap on the right shows the number of revisit overpasses in a 24 hours period. The CIMR mission is specifically designed to ensure sub-daily coverage in all the Arctic region. In particular, CIMR will achieve full sub-daily, contiguous coverage of the pan-Arctic region. By symmetry, the coverage is also excellent in the Antarctic region. Over 95% of the globe will be covered on a daily basis (Lavergne, T., Pinol Sole, M. and Donlon, C.: Daily coverage of CIMR (Arctic, Antarctic, and Global views), figshare, doi:10.6084/m9.figshare.7749284.v1, 2019).

Over the Polar Regions, by combining the capability of both CIMR and MetOp-SG(B) MWI/ICI, measurements spanning a large microwave spectrum between 1.4 to 664 GHz will be available for the first time, CIMR will deploy a wide-swath (>1900 km) conically scanning multi-frequency microwave radiometer. Technical requirements for the CIMR mission are provided in Table 1. Measurements will be made using a forward scan arc followed ~260 seconds later by a second measurement of the same location using a backward scan arc. Full Stokes vector output is included in the mission design for channels centred at 1.4135, 6.925, 10.65, 18.7 and 36.5 GHz.

High spatial resolution (<5 km) is required at L1b for Ka-band channels (to attain an equivalent performance to AMSR2 89 GHz measurements of SIC) and ≤15 km for SST: both demand a large diameter, rotating, deployable wire mesh antenna with performance up to Ka-band frequencies. The advantage of using low frequency measurements for SIC is that atmospheric effects are less pronounced at Ka-band than at 89 GHz. For L-band and C-band channels a highly performant NEΔT requirement is set since retrieval of SST and sea surface salinity in cold Arctic waters are limited by NEΔT. L-band is used to determine sea surface salinity, ocean winds and soil moisture (amongst other products). All channels are oversampled by ≥20% in the scan and flight direction except the Ku band where contiguous samples are permitted and at the Ka-band where gaps ≤1 km are permitted. For CIMR, Absolute Radiometric Accuracy (ARA) is not used in the traditional manner but instead, we calculate the Total Standard Uncertainty (which is a "zero mean, 1-sigma" total uncertainty). This offers a better practical approach when validating requirements. Demanding L1b stability requirements set over the mission lifetime are specified to ensure that appropriate stability in the long-term climate record. If a second satellite is added to the CIMR mission, a dedicated time-limited tandem flight will be flown in which both satellites will be on the same orbit separated by 30-60 seconds in time (to minimise the impact of atmospheric and ocean variability) to ensure that the long-term climate record is stable.

As planned, the performance of CIMR means that it could be used to monitor the calibration of other concurrently flying missions using Simultaneous Nadir Overpasses or other methods. Figure 3 highlights the ground processing approach and major products foreseen from the CIMR mission.

Return to Page One

doi: 10.25923/ymt5-wz59

Channel centre frequency[1] [GHz]	1.4135	6.925	10.65	18.7	36.5
Maximum channel bandwidth [MHz]	27	825	100	200	1000
L1b spatial resolution [km] (computed as the mean of the major and minor axis of the projected channel footprint on ground)	<60 (SMAP: 40)	≤15 (AMSR2: 48)	≤15 (AMSR2: 33)	≤5.5 (AMSR2: 18)	<5(goal 4) (AMSR2: 9)
L1b Radiometric resolution [K] NEΔT for zero mean, 1 sigma at 150 K	≤0.3 (SMAP: 0.93)	≤0.2 (AMSR2: 0.3)	≤0.3 (AMSR2: 0.6)	≤0.4(goal:0.3) (AMSR2: 0.6)	≤0.7 (AMSR2:0.6)
Dynamic Range [K]	Kmin=2.7, Kmax=340				
L1b Radiometric Total Standard Uncertainty [K, zero mean, 1 sigma)]	≤0.5	≤0.5 (goal ≤0.4)	≤0.5 (goal: ≤0.45)	≤0.6 (goal: ≤0.5)	≤0.8
Polarisation	Full Stokes.				
Swath width [km]	>1900				
Observation Zenith Angle [deg]	55.0 ±1.5. (SMAP: 40, AMSR2: 55)				
L1b Radiometric stability over lifetime [K, zero mean, 1 sigma]	≤0.2	≤0.2	≤0.2	≤0.2	≤0.2
L1b Radiometric stability over *orbit* [K, zero mean, 1 sigma]	≤0.2	≤0.15 (goal=0.1)	≤0.15 (goal=0.1)	≤0.2	≤0.2
L1b geolocation uncertainty [km]	≤1/10 of L1b measurement spatial resolution				
Applications**	SIT, SIC, SSS, WS, SM, SD	SIC, SST, SIT, IST, WS, SID, SM, SD	SST, PCP, WS, SD, SM	TWV, TCWV, PCP, SIC, SD, SM, SID	SIC, SST, TWV, TCWV, PCP, SIC, SWE, SD

***SIC = Sea Ice Concentration, SST = Sea Surface Temperature, SIT = Sea Ice thickness, SSS= Sea Surface Salinity, WS = Wind speed, TWV = Total Water Vapour, TCWV = Total Cloud-liquid Water Vapour, SD = Snow Depth on sea ice, SM = Soil Moisture, SWE = Snow Water Equivalent, SID = Sea Ice Drift, PCP=precipitation)*

Table 1. Key Mission Requirements for the CIMR mission (From Donlon, 2019).

L1a and L1b products are provided in native scan geometry whereas L1c and L2 products are gridded format. Inter-comparison with other satellite systems within the GSICS framework will be an extremely useful part of the mission verification process once on-orbit. The CIMR project completed its preparatory phase (Phase A/B1) that started in 2018 under the guidance of ESA and is preparing mission implementation (Phase B2/C/D/E1) starting in 2020. A first launch no earlier than the 2027/28 timeframe. CIMR will provide Copernicus

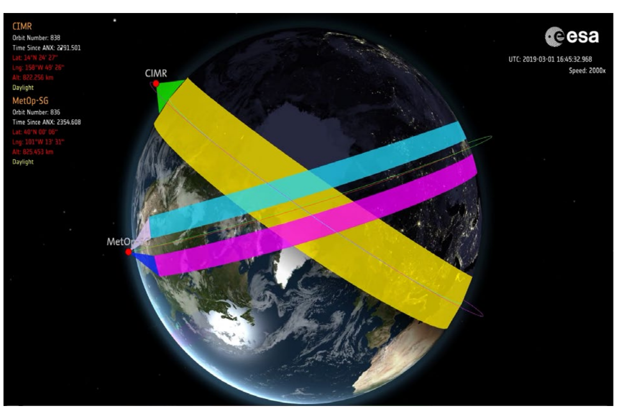

Figure 2. CIMR and MetOp-SG(B1) fly in loose formation such that the difference between CIMR and MetOp-SG(1B) scatterometer measurements are within +/-10 minutes of each other in the Polar Regions.

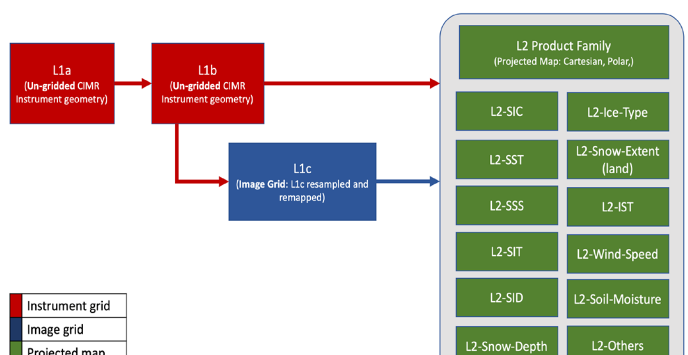

Figure 3. Schematic overview of the main data products for the CIMR mission.

[1] The channel center frequency is not necessarily the same as the ITU EESS (passive) allocated band centre frequency.

Return to Page One

doi: 10.25923/ymt5-wz59
GSICS Quarterly: Winter Issue 2020 Volume 13, No. 4, 2020

with unprecedented views of the Polar Regions at a time when Arctic summer sea ice is anticipated to be considerably reduced compared to present conditions leading to profound changes. The global coverage provided by CIMR provides a fundamental capability underpinning Copernicus service needs.

References

Donlon, C. J., 2019, the Copernicus Imaging Microwave Radiometer (CIMR) Mission Requirements Document, ESA-EOPSM-CIMR-MRD-3236, Version 3, available at https://www.esa.int/Applications/Observing_the_Earth/Copernicus/Copernicus_High_Priority_Candidates

Discuss the Article

Py4CAtS: PYthon for Computational ATmospheric Spectroscopy

By Franz Schreier and Philipp Hochstaffl, DLR

Radiation is a key for many branches of physics. In the atmospheric sciences radiative transfer (RT) is crucial for weather and climate, and RT modeling is mandatory for remote sensing [e.g. Zdunkowski et al., 2007]. Accordingly a vast number of RT models (RTM) has been developed in the past, spanning the ultraviolet, infrared (IR), to microwave (MW) spectral range. For high resolution spectroscopy in the IR and MW, line-by-line (lbl) modeling of molecular absorption is mandatory. Lbl models are also indispensable for generation and verification of fast parameterized models.

Radiative transfer depends on spectral range, geometry, atmospheric pressure, temperature, and composition, and the optical properties of molecules and particles. Molecular absorption is characterized by the superposition of individual lines where the data is taken from compilations such as HITRAN or GEISA [Gordon et al., 2017, Jacquinet-Husson et al., 2016] comprising parameters (position, strength, broadening parameters etc.) for million to billion of lines of some dozen molecules. Most RTMs incl. lbl models are used as a kind of "black-box", i.e. the code reads all settings and auxiliary data from input file(s) and delivers spectra (radiance, transmission etc.) as output. This is clearly advantageous for modeling a large number of spectra, but for detailed analysis of the physical processes inspection of intermediate variables can be helpful.

Py4CAtS has been developed with this intention [Schreier et al., 2019]. In essence it is a Python re-implementation of the Fortran Generic Atmospheric Radiation Line-by-line Code GARLIC, [Schreier et al., 2014] where compute-intensive code sections utilize Numeric/Scientific Python modules for highly optimized array-processing [van der Walt et al., 2011, Langtangen, 2008, Lin, 2012]. The individual steps of an IR or microwave RT computation are implemented in separate modules and functions (Fig. 1):

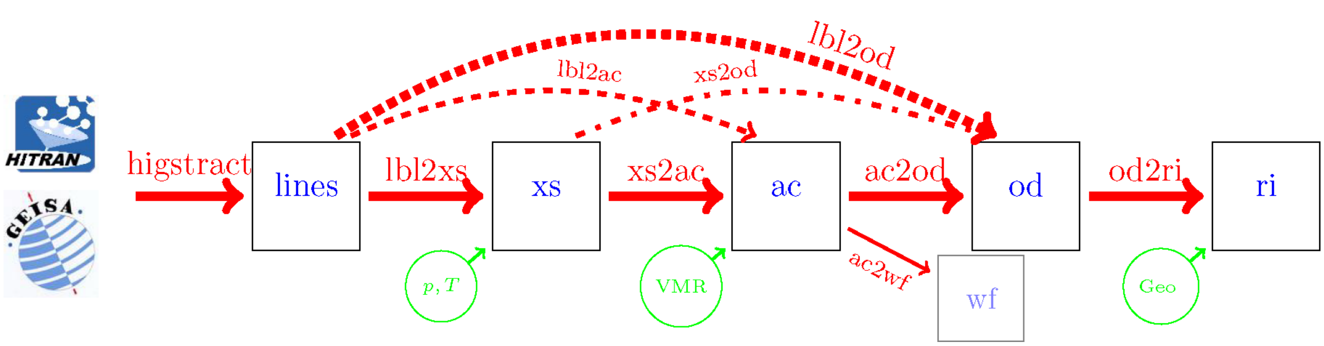

Figure 1: From Hitran/Geisa via cross sections (xs) and absorption coefficients (ac) to optical depths (od) and radiation intensity (ri). Cross sections are pressure and temperature (pT) dependent, absorption coefficients also depend on composition (volume mixing ratio), and optical depth and radiance depend on path geometry. Weighting functions (wf) are available, too.

Return to Page One

doi: 10.25923/ymt5-wz59

- to extract lines of relevant molecules in the spectral range of interest,
- to compute lbl cross sections for given pressure(s) and temperature(s),
- to combine cross sections to absorption coefficients and optical depths and
- to integrate along the line-of-sight to transmission and radiance/intensity.

Here, absorption cross sections are the computationally most demanding step. As default Py4CAtS considers a Voigt line profile accounting for pressure and Doppler broadening, and utilizes highly optimized algorithms [e.g. Schreier, 2006, 2011, 2018].

The recommended way to use Py4CAtS is the IPython [Pérez and Granger, 2007] shell/notebook (alternatively it can be used from the Unix shell) and Fig. 2 exemplifies a typical session. The first block demonstrates how to read atmospheric data. **`atmRead`** returns a so-called "structured NumPy array", a kind of matrix with rows corresponding to atmospheric levels, and columns accessible by names (e.g., 'p', 'T', or 'H2O') instead of numbers (see the third call of **`lbl2xs`** in the In [4]: block). Next line parameters of the five main IR absorbers in the 5 µm region are read from the GEISA database using the **`higstract`** function. The **`atmPlot`** and **`atlas`** functions are then used to plot the data.

To get an idea about the CO absorption, the cross section (xs) is calculated next for the GEISA (or HITRAN) database reference pressure and temperature (1 atm, 296 K). The impact of pressure is explored with the second call of the **`lbl2xs`** function. Finally, cross sections of all five molecules and all levels of the midlatitude-summer atmosphere are calculated. The results are then visualized using the **`xsPlot`** function.

The sum of all cross sections scaled by the molecule's number density gives the absorption coefficient (ac). This step (including appropriate interpolation) is performed by the **`xs2ac`** function level-by-level. In the following step the absorption coefficients are integrated by **`ac2dod`** to compute the vertical delta (or layer) optical depths (od): the result is a list of optical depths, one for each atmospheric layer (defined by the lower and upper levels). **`dod2tod`** can be used to sum up all layer optical depths to the total optical depth, the integral of the absorption coefficient from bottom- to top-of-atmosphere. As indicated in Fig. 1, the intermediate steps can be bypassed and the optical depth can be calculated with atmospheric and line data as input using the **`lbl2od`** function (see the In [6]: block of Fig. 2).

```
Jupyter QtConsole 4.3.1
Python 3.6.9 (default, Oct 29 2019, 10:39:36) [GCC]

In[1]: # get two mid latitude atmospheres
  ...: mls = atmos1D('/data/atmos/20/mls.xy')
  ...: mlw = atmos1D('/data/atmos/20/mlw.xy', zToA=50)

Atmos1d: got p, T, air and 7 gases at 20 levels
Atmos1d: got p, T, air and 7 gases at 16 levels

In [2]: # IASI microwindow for CO retrieval: HItran-GeiSa-exTRACT
   ...: dictLineLists = higstract('/data/geisa/87/lines',
                                  (2100,2150), molecule='main')
9771  lines of  5  molecule(s), returning a dictionary

In [3]: atmPlot(mls);  atmPlot([mls,mlw], 'O3', 'mb')
   ...: atlas(dictLineLists) # plot line data (default strength)
```

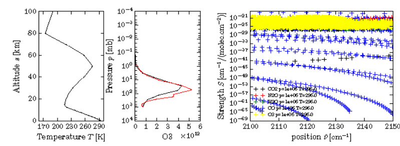

```
In [4]: # CO cross section at database pressure and temperature
   ...: xs  = lbl2xs(dictLineLists['CO'])
   ...: # a list of cross sections for three pressures
   ...: xss = lbl2xs(dictLineLists['CO'], [1013,100,10,'mb'])
   ...: # a dictionary of x-section lists (for all p, T, gases)
   ...: xssDict = lbl2xs(dictLineLists,mls['p'],mls['T'])
   ...: # ... and some plots (not all are shown here)
   ...: xsPlot(xs);  xsPlot(xss);  xsPlot(xssDict)
```

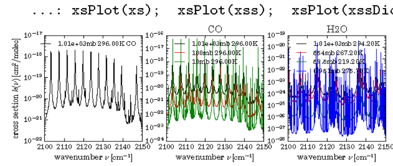

```
In [5]: # proceed step-by-step
   ...: acList  = xs2ac(mls, xssDict) # absorption coefficients
   ...: dodList = ac2dod(acList)      # delta optical depths

In [6]: # alternatively bypass intermediate quantities, e.g.
   ...: dodList = lbl2od(mls,dictLineLists)  # delta opt.depths

In [7]: # sum/combine optical depths and plot
   ...: odPlot([dodList[0], dodList[1]])  # the bottom layers,
   ...: odPlot(dodList[0]+dodList[1])     # ... their sum,
   ...: odPlot(dod2tod(dodList))          # and total opt.depth
```

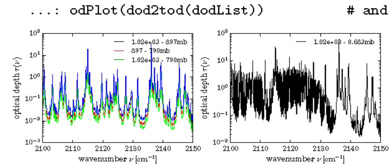

```
In [8]: # radiation intensity seen by uplooking observer at BoA
   ...: radUp = dod2ri(dodList)
   ...: # downlooking at ToA (incl. surface @ 294K) Gauss-convolved
   ...: radNadir = dod2ri(dodList, 180, 294.2).convolve(1.0,'G')
```

Figure 2: Typical workflow of Py4CAtS. Output is not shown except for the first two commands.

Return to Page One

Finally, radiance/intensity can be computed both for up and downlooking observation geometries, optionally convolved with a box, triangular or Gaussian response function (default box with width 1 cm^{-1}).

All spectral quantities are stored internally as “subclassed” NumPy arrays, where in addition to the spectrum further information is stored as attributes: wavenumber interval, pressure, temperature, etc. (e.g. **`xs.x, xs.molec, od.p, . . .`**). In addition to the quick-looks the data can be saved to and read from files with appropriate functions (e.g. **`xsRead, odSave`**). Most of these plot, read, and save functions work recursively, i.e. they can be called with a single “spectrum” or a list thereof.

The main objective for Py4CAtS has not been a highly efficient and accurate lbl radiative transfer code; the performance of the GARLIC Fortran code vs. Py4CAtS is discussed in subsection 4.4 of Schreier et at. [2019].
The continued speed-up of NumPy is also discussed in section 4 of Schreier [2018]. The package is intended to complement rather than to compete with well-known codes such as ARTS [Eriksson et al., 2011, Buehler et al., 2018], FASCODE/LblRTM [Clough et al., 2005], GenLN2 [Edwards, 1988], or RFM [Dudhia, 2017]. Nevertheless, despite the speed limitations of interpreters such as Python and the neglect of continua or scattering Py4CAtS, is believed to be attractive because it is flexible, versatile, and easy to use. A tarball of the Python source files is available at our department’s server at https://atmos.eoc.dlr.de/tools/Py4CAtS/.

Return to Page One

References

Buehler. S. A et al . ARTS, the atmospheric radiative transfer simulator – version 2.2, the planetary toolbox edition. *Geosci. Model Dev.*, 11: 1537–1556, 2018. doi: 10.5194/gmd-11-1537-2018.

S.A. Clough, et al. Atmospheric radiative transfer modeling: a summary of the AER codes. *J. Quant. Spectrosc. & Radiat. Transfer*, 91(2):233–244, 2005. doi: 10.1016/j.jqsrt.2004.05.058.

A. Dudhia. The reference forward model (RFM). *J. Quant. Spectrosc. & Radiat. Transfer*, 186:243–253, 2017. doi: 10.1016/j.jqsrt.2016.06.018.

D.P. Edwards. Atmospheric transmittance and radiance calculations using line–by–line computer models. In *Modelling of the Atmosphere*, volume 928, pages 94–116. Proc. SPIE, 1988. doi: 10.1117/12.975622.

P. Eriksson, et al. ARTS, the atmospheric radiative transfer simulator, version 2. *J. Quant. Spectrosc. & Radiat. Transfer*, 112(10):1551–1558, 2011. doi: 10.1016/ j.jqsrt.2011.03.001.

I.E. Gordon, L.S. Rothman, et al. The HITRAN2016 molecular spectroscopic database. *J. Quant. Spectrosc. & Radiat. Transfer*, 203:3 – 69, 2017. doi: 10.1016/j.jqsrt.2017.06.038.

N. Jacquinet-Husson et al. The 2015 edition of the GEISA spectroscopic database. *J. Mol. Spectrosc.*, 327:31 – 72, 2016. doi: 10.1016/j.jms.2016.06.007.

Langtangen, H.P. *Python Scripting for Computational Science*, volume 3 of *Texts in Computational Science and Engineering*. Springer, 3 edition, 2008. doi: 10.1007/978-3-540-73916-6.

Johnny Wei-Bing Lin. Why Python is the next wave in earth sciences computing. *BAMS*, 93(12):1823–1824, 2012. doi: 10.1175/BAMS-D-12-00148.1.

Pérez, F. and B.E. Grange IPython: a system for interactive scientific computing. *Computing in Science & Eng.*, 9(3):21–29, May 2007. doi: 10.1109/MCSE.2007.53. URL https://ipython.org.

F. Schreier. Optimized evaluation of a large sum of functions using a three-grid approach. *Comp. Phys. Comm.*, 174:783–802, 2006. doi: 10.1016/j.cpc.2005.12.015.

F. Schreier. Optimized implementations of rational approximations for the Voigt and complex error function. *J. Quant. Spectrosc. & Radiat. Transfer*, 112(6):1010–1025, 2011. doi: 10.1016/j.jqsrt.2010. 12.010.

F. Schreier. The Voigt and complex error function: Humlíček’s rational approximation generalized. *Mon. Not. Roy. Astron. Soc.*, 479(3):3068–3075, 2018. doi: 10.1093/mnras/sty1680.

F. Schreier, et al. GARLIC – a general purpose atmospheric radiative transfer line-by-line infrared-microwave code: Implementation and evaluation. *J. Quant. Spectrosc. & Radiat. Transfer*, 137:29–50, 2014. doi: 10.1016/j.jqsrt.2013. 11.018.

F. Schreier, S. Gimeno García, P. Hochstaffl, and S. Städt. Py4CAtS — PYthon for Computational ATmospheric Spectroscopy. *Atmosphere*, 10(5):262, 2019. doi: 10.3390/atmos10050262.

S. van der Walt, et al. The numpy array: A structure for efficient numerical computation. *Computing in Science & Eng.*, 13(2):22–30, 2011. doi: 10.1109/MCSE.2011.37.

W. Zdunkowski, et al. *Radiation in the Atmosphere — A Course in Theoretical Meteorology*. Cambridge University Press, 2007.

Discuss the Article

doi: 10.25923/ymt5-wz59

GOES Calibration and Operation

By Xiangqian Wu Fangfang Yu and Vladimir Kondratovich, NOAA

This is a brief review of recent Geostationary Operational Environmental Satellite (GOES) earth imaging instrument calibration and operations.

GOES-13 has been an on-orbit backup at 60°W since it was retired from GOES-EAST duty in January 2018. In Feb 2020, it arrived at its new duty station to support the Indian Ocean mission. Before its drift in July 2019, NOAA verified that its calibration was nominal. After nearly 14 years of on-orbit storage and operation, GOES-13 has low fuel reserve for station keeping, and will operate as Extended GOES in High Inclination (XGOHI).

GOES-15 moved to 128°W in November 2018, and has been operating there for users to evaluate whether GOES-17 can serve as GOES-WEST alone. This operation ended in March 2020. GOES-15 has joined GOES-14 in healthy on-orbit storage.

GOES-16 serves as GOES-East at 75.2°W since 18 December 2017. GOES-17 serves as GOES-West at 137.2°W since 12 February 2019. The key payload on these satellites is the Advanced Baseline Imager (ABI). The Level 1b (calibrated and navigated radiance) and Cloud and Moisture Imagery (CMI) products reached the Full Validation maturity on 1 June 2018 for GOES-16 and on 19 February 2020 for GOES-17. Figures 1-3 summarize key performance of these ABIs; the GOES Calibration website has more details. GOES-16 performs well in all aspects. GOES-17 infrared channels have higher noise because of the partial failure of its cooling subsystem, but it meets the waived requirement most of the time. The accuracy and INR performance are not affected. The higher bias for Channel 16 is due to the change of its spectral response function at higher operating temperature; it will be revised in the near future.

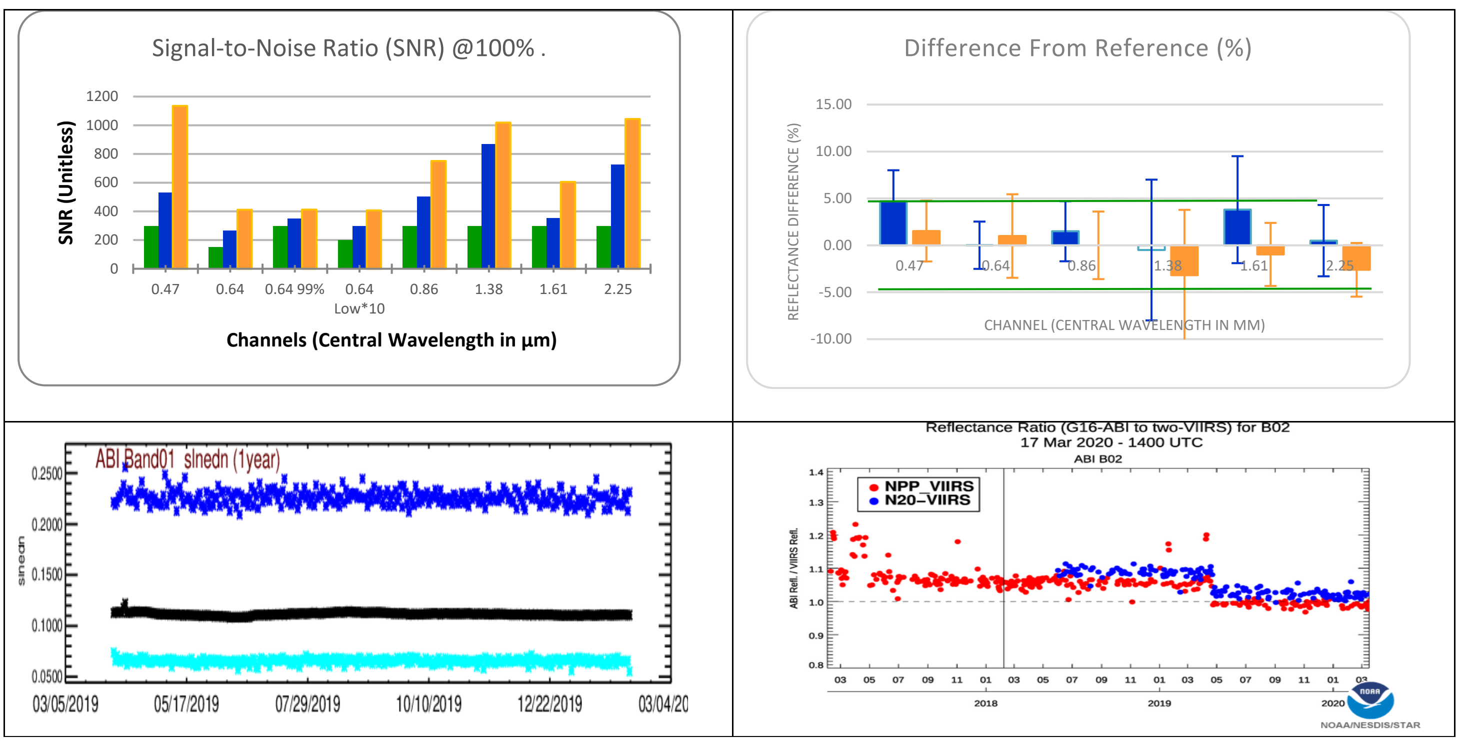

Figure 1: Visible and Near Infrared (VNIR) channels performance: Noise (Signal-to-Noise Ratio or SNR, upper left), accuracy (difference from VIIRS corresponding channels, upper right), and their stability (lower row). In upper row, green, blue, and orange bars are requirement and performance of GOES-16 and GOES-17, respectively. The requirement is minimum for GOES-16, and waived to average for GOES-17. For the 0.64 µm channels, there are requirements for all detectors (left), for the best 99% of detectors, and for SNR at 5% reflectance. In the lower left panel, the cyan, black, and blue symbols are, respectively, minimum, average, and maximum of all detectors.

Return to Page One

doi: 10.25923/ymt5-wz59

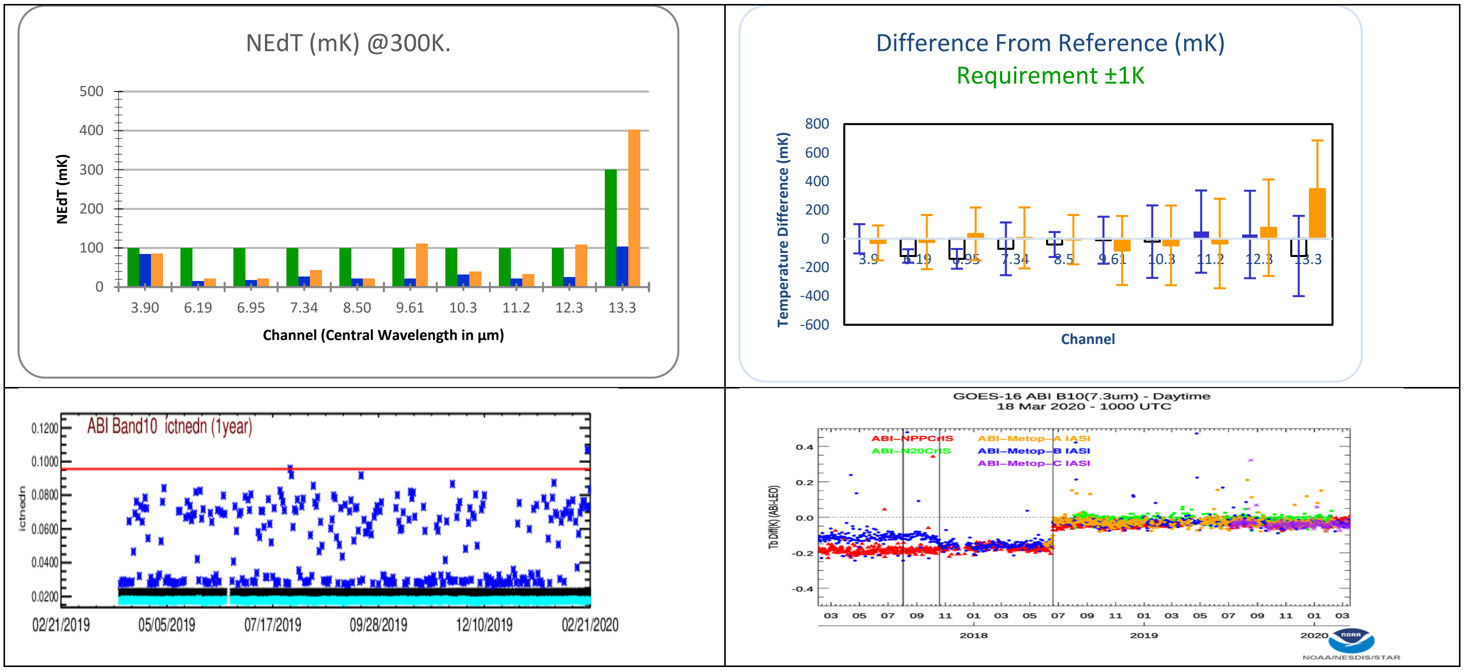

Figure 2: Infrared (IR) channels performance: Noise (Net Equivalent Differential Temperature or NEdT, upper left), accuracy (difference from hyperspectral sounders, upper right), and their stability (lower row). In upper row, green, blue, and orange bars are requirement and performance of GOES-16 and GOES-17, respectively. The requirement is maximum for GOES-16, waived to average for GOES-17, and further waived to 0.12K and 0.37K for the 9.61 µm and 13.3 µm channels, respectively (not shown in chart). For GOES-17, the performance is evaluated during the relatively cool and stable period of the day. In the lower left panel, the cyan, black, and blue symbols are, respectively, minimum, average, and maximum of all detectors, and the red line is requirement.

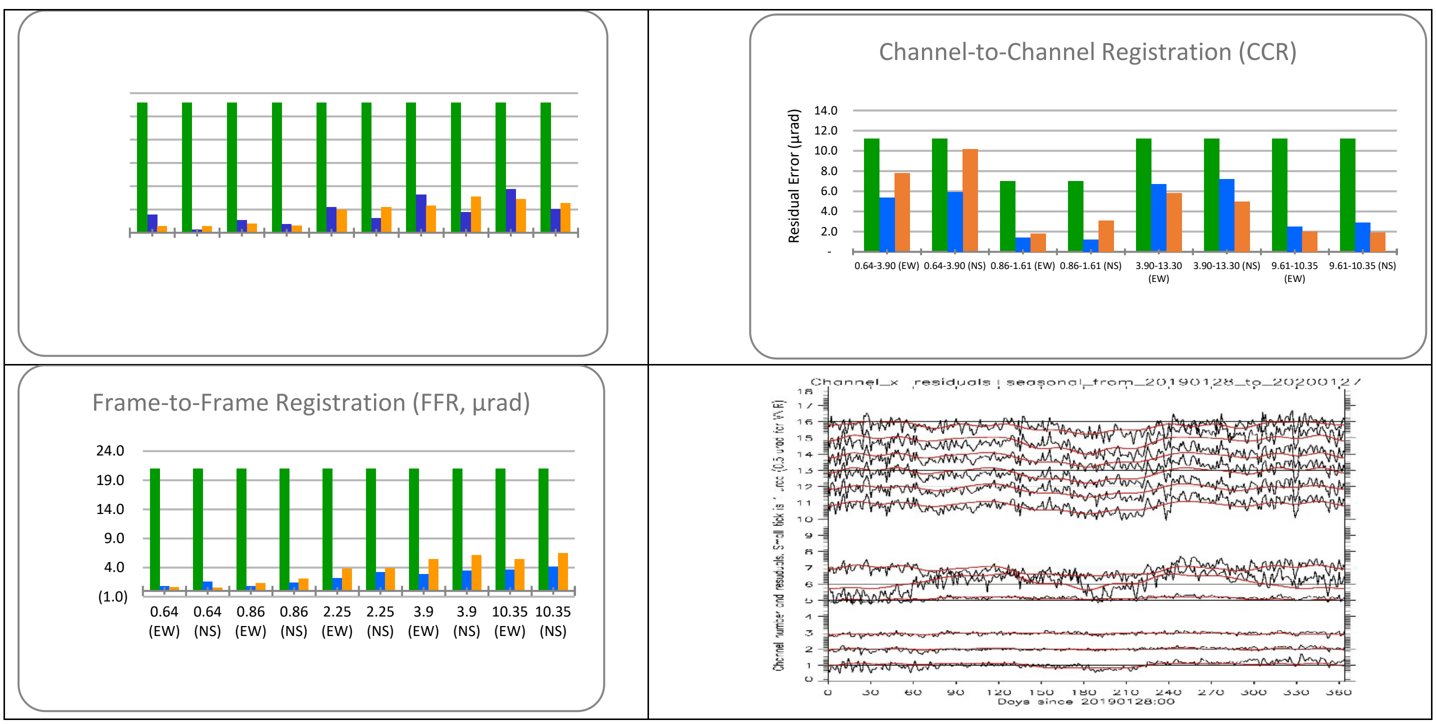

Figure 3: Image Navigation and Registration (INR) performance: Navigation error for representative channels (upper left), Channel-to-Channel Registration errors (CCR, upper right), Frame-to-Frame Registration errors (FFR, lower left), and East-West navigation error of GOES-17 for one year (lower right) as an example of INR stability. The green, blue, and orange bars are requirement and performance of GOES-16 and GOES-17, respectively. In the lower right panel, the number on the right indicates the ABI channel; note the missing data for Channels 4 and 8-10 that cannot be directly evaluated due to atmospheric absorption.

Return to Page One Discuss the Article

doi: 10.25923/ymt5-wz59

NEWS IN THIS QUARTER

Summary of the First ISCCP-NG Workshop

By Andrew Heidinger, NOAA

The Next Generation of the International Satellite Cloud Climatology Project (ISCCP-NG) is proposed as a follow-on to the classic ISCCP which would commence in 2022 once the EUMETSAT Meteosat 3rd Generation (MTG) is launched. Once MTG is operational, the entire geostationary ring will be encircled by imagers which offer capabilities far superior to those from the previous generation of imagers. These sensors will provide full-disk scans every 10-15 minutes with roughly 12 common channels and with spatial resolutions of 2km for thermal channels and finer spatial resolutions for selected solar channels. This data volume and fidelity represent a significant advance beyond that available at the start of ISCCP in the early 1980's. The challenge facing ISCCP-NG is to define a new baseline from this data and processing methods to extract meaningful information for the scientific community in the coming decades.

EUMETSAT hosted the first workshop addressing the next generation of cloud climatology following the current ISCCP and other data records on 28-30 October 2019, at the EUMETSAT Facility in Darmstadt, Germany. The project is primarily named the Next Generation of the International Satellite Cloud Climatology Project (ISCCP-NG). Currently, ISCCP is a project that reports to the GEWEX Data and Analysis Panel (G-DAP), led by Remy Roca and Tristan L'Ecuyer. Andrew Heidinger, a member of G-DAP, was tasked with organizing this workshop. Jörg Schulz (EUMETSAT) served as local host. The organizing committee also included Graeme Stephens who represented the GEWEX Science Steering Group and Brian Kahn from NASA JPL. Roughly 50 people were invited to this workshop and roughly 40 people attended with several calling into the meeting. Attendees represented EUMETSAT, NOAA, JMA, CMA and KMA space agencies and NASA research agencies. In addition, researchers in the ESA Climate Change Initiative project on cloud climatology were present. The workshop was organized around a plenary session and four breakout groups (Input, Output, Applications and Governance). The summaries of the breakout groups are reported below and are captured in full in the document archive for this meeting

Input (Radiometric issues and generation of homogenized L1 data) Group Summary:

- The Global Space-based Inter-Calibration System (GSICS) is optimistic that it can fulfill the radiometric calibration needs

Group Photograph taken October 28, 2019 by EUMETSAT management

Participants of the ISCCP-NG Workshop

Return to Page One

doi: 10.25923/ymt5-wz59

for the new geostationary instruments. However, the new cloud property data records shall be consistent with past data, which requires a more holistic view to the full time series of geostationary data including a full re-calibration of all geostationary data to today's standards, e.g.., including uncertainty estimates. A thorough discussion how space agencies participating in GSICS can achieve this needs to take place in the GSICS Research Working Group at its next meeting.

- No consensus was obtained on the spectral, spatial and temporal sampling to construct a new baseline ISCCP-NG data set. Arguments were made in favor of using the 12 common channels on a common grid of 4 km and temporal resolution of 30 minutes. Other arguments were made to make no subsetting choice and let L2 algorithms make those decisions. Determination of the ISCCP-NG baseline will require investigation of various prototypes prior to the next workshop.

Output (Generation of L2 and L3 data) Group Summary:

- ISCCP-NG's potential product list should be guided by the intended Applications but is expected to grow well beyond that available from ISCCP.
- Ability to make products consistent with past cloud climatology such as from ISCCP and other data records is critical.
- For the beginning of ISCCP-NG, the idea of an ensemble approach to L2 creation is desired. A strict list of requirements for any ensemble member is needed.
- L2 creation should take advantage of actual trends in data processing such as cloud computing and on-demand processing techniques aiming at a minimum need for data repatriation
- A further aim of an intelligent data processing approach is a synergy with aerosol climate data processing that should be explored as well.

Applications (Users of ISCCP-NG Data and connection to the external community) Group Summary:

- The Applications Breakout Group came up with four scientific themes for ISCCP-NG
- Ensure cloud climatology continuity: ISCCP-classic and other existing cloud property data records. To utilise past data in an optimised way a reprocessing of past data is not excluded
- Global multi-scale (time and space) process understanding of dynamics of cloud, radiation, and precipitation
- Global multi-scale (time and space) process understanding of aerosol, cloud, and precipitation interactions
- Global multi-scale (time and space) process understanding of high impact, societally relevant weather, hydrological cycle events, and air quality
- A first version of a science traceability matrix linking scientific questions with needed sensor data and activities was created based on the workshop discussions. This needs to be extended to all relevant application to be addressed.

Governance Group Summary:

- The current governance for the ISCCP was reviewed and it is evident that while MoU's were appropriate for ISCCP since agencies only transferred data, the new project will require more regulations and therefore MoUs between individual agencies may not be suitable
- The new project should be considered a project within an international framework close to space agencies. WMO GSICS and SCOPE-CM coordination mechanisms may host such projects and CEOS/CGMS WGClimate and GEWEX SSG may be suitable bodies providing oversight. It is of high importance that agencies make real commitments beyond the best effort to enable a plan for this likely decade long project. Once the planning contains specific data records those should be added into the planned category of the CEOS/CGMS WG Climate GCOS ECV Climate Data Record Inventory.

Next Steps: A report is being written for CGMS 48 on 24-29 May, 2020 (dates and location are uncertain due to the COVID-19) The purpose of this report is to engage the space agencies, in particular for the reprocessing of geostationary radiance data, and to develop a terms of reference for the new project and its relationship to other international bodies. A Topical Group has been added to the CGMS International Cloud Working Group (ICWG). This TG will discuss the L1

Return to Page One

doi: 10.25923/ymt5-wz59

and L2 issues raised at the ISCCP-NG workshop. In particular, Martin Stengel (DWD), Ken Knapp (NESDIS/NCEI) and Andrew Heidinger (NESDIS/STAR) will generate sample L1g and L2 data and lead discussions on the optimal L1 and L2 spatial, spectral and temporal sampling. The next annual meeting of GSICS has been postponed to spring 2021, but GSICS will devote time to discuss what GSICS can achieve for ISCCP-NG and report back to the ISCCP-NG organizing panel. After reviewing the feedback from the above activities, a 2nd Workshop will be planned for some time in 2021.

Program Committee Andrew Heidinger (NOAA/SSEC), Tristan L'Ecuyer (Univ. Wisconsin-Madison/SSEC), Jörg Schulz (EUMETSAT), Remy Roca (LEGOS), Brian Kahn (NASA/JPL), and Graeme Stephens (GEWEX and A-CCP)

Workshop Website: https://www.ssec.wisc.edu/meetings/isccp-ng/2019-meeting/

Discuss the Article

Geostationary Satellite for Monitoring Asian Air Quality and Ocean Environment (GeoKOMPSAT-2B) Launched on 19 February 2020

By Won Jun Choi, National Institute of Environmental Research (NIER)

GeoKOMPSAT-2B (GK2B) was launched on 19 February 2020 from French Guiana. This satellite is the one of Korea's Geostationary Multi-purpose Satellite series and its mission is to observe Asian air quality and ocean environment focusing on the Korean peninsula and the surroundings for the next ten years. GK2B is equipped with two important instruments: the Geostationary Environment Monitoring Spectrometer (GEMS) and the Geostationary Ocean Color Imager-2 (GOCI-2).

GEMS is a hyper-spectrometer to monitor air quality in the 300~500 nm spectral range with 0.2 nm resolution and 0.6 nm full width at half maximum (FWHM), and the measured spectra will be used to estimate atmospheric pollutants such as NO_2, SO_2, HCHO, O_3, and aerosols. GEMS field of regard (FOR) covers from Japan in the east to northern Indonesia and southern Mongolia in the west, with 7 x 8 km^2 (at Seoul) Ground Spatial Distance (GSD). GEMS will nominally scan its domain 8 times per day during daylight. Air quality data retrieved from GEMS is expected to be available from early 2021.

The National Institute of environmental Research (NIER) of the Ministry of Environment, in charge of development, operation and data production/management/distribution of GEMS, plans to conduct joint research for calibration and validation as GEMS is the first of its kind to observe air quality from geostationary orbit. NIER will open an announcement of opportunity (AO) call for GEMS calibration and validation in late March to recruit international researchers (For more details, see the GEMS website http://nesc.nier.go.kr).

GOCI-2 will take over the current ocean mission of the Communication, Ocean and Meteorological Satellite (COMS), or GK1, launched in 2010. GOCI-2 has much improved performance – four times higher ground resolution: from 500m to 250m, double the number of products: from 13

	GEMS	GOCI 2
GSD	7 x 8 km^2	Local : 250m (Nadir) Global: 1,000 m
Number of Channels	1,000 (300 - 500 nm, with 0.2 nm)	13 (visible: 9, NIR: 3, Broadband: 1)
Observation cycle	8 times/day	Local: 10 times/day Global: 1 time/day
Observation time	For 30 minutes from the :45 of each hour	For 30 minutes from the :15 of each hour
Field of regard	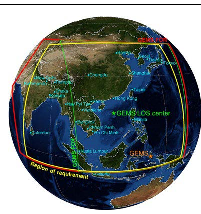	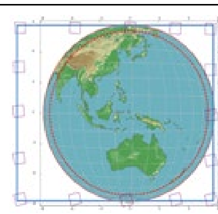 Global 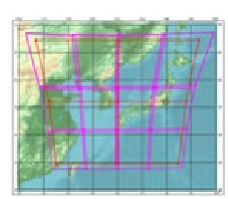 Local

doi: 10.25923/ymt5-wz59

to 26 items, more wavelengths: from 8 to 13, and more frequent observations: from 8 to 10 times per day.

GOCI-2 will continuously monitor ocean pollutants, such as red/green algae, oil spills and waste, that could cause a significant adverse impact on the marine environment. Moreover, with its ability to observe diverse ocean characteristics including sea fog, sea ice, and salinity, GOCI-2 is expected to contribute to a wide range of ocean related studies. Ocean data from GOCI-2 will be available to the public as early as October 2020 (See http://kosc.kiost.ac.kr/eng. GOCI data has been accessible since 2010).

References

Cho, S., et al., Korean Program. Comprehensive Remote Sensing (2018), vol. 1, pp. 299–339. Oxford: Elsevier.

Choi, W. J. et al., Introducing the Geostationary Environment Monitoring Spectrometer. J. Appl. Remote Sens. 12(4), 044005 (2018), doi: 10.1117/1.JRS.12.044005.

Coste, P. et al., Development of the new generation of geostationary ocean color imager, Proc. SPIE (2017), 10562, 105620D.

Kim, H. O. et al., Space-based earth observation activities in South Korea, IEEE Geosci. and Remote Sens. (2015), 3(1), 34–39

Discuss the Article

Announcements

Third Joint GSICS/IVOS Lunar Calibration Workshop – Darmstadt, Germany, 16-19 November 2020

By S. Wagner (EUMETSAT), T. Stone (USGS), X. Hu (CMA), X. Wu (NOAA) and V. Mattioli (EUMETSAT)

In order to fulfil more and more demanding radiometric requirements, Earth Observing satellite instruments need to deploy complex systems either on board or on the ground for their calibration and the monitoring of their temporal stability. In the reflective part of the solar spectrum, the latest generations of radiometers aboard geostationary and polar satellites also expand their spectral coverage, typically from 0.4µm to 2.3µm.

In that context, lunar calibration is the most powerful method to address both calibration and monitoring needs aside on-board calibration units.

In the recent years, significant efforts have been made to promote and develop lunar calibration activities within GSICS and CEOS WGCV IVOS. A first joint Lunar Calibration Workshop was organised in December 2014 and led to the endorsement by the Lunar Calibration Community of the GSICS Implementation of the ROLO (GIRO) model as the established publicly-available reference for lunar calibration of reflective solar bands.

In November 2017, a second joint workshop continued this initial effort, putting emphasis on dedicated lunar measurement campaigns, developments of radiance models, and new algorithms to develop new lunar inter-calibration products. This second event was also an opportunity to look at alternative

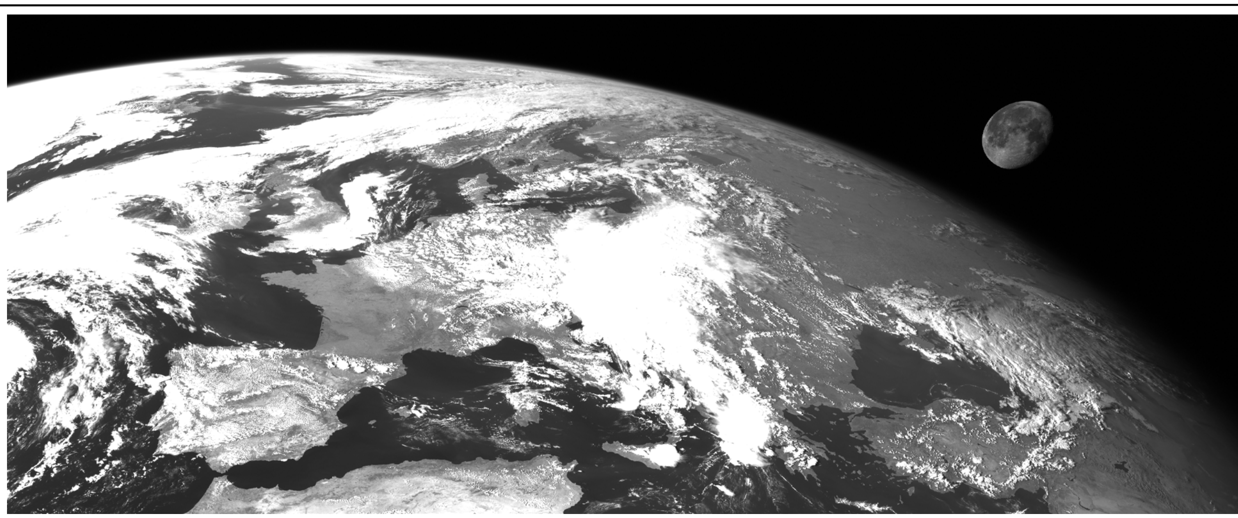

Return to Page One

usages of lunar imagery such as the post-launch characterisation of Modulation Transfer Functions or to liaise with other communities having a strong interest in lunar calibration, in particular the microwave community.

In order to share knowledge and expertise on lunar calibration, the Third Joint GSICS/IVOS Lunar Calibration Workshop will be hosted by EUMETSAT in Darmstadt, Germany, 16-19 November, 2020 and organised jointly by EUMETSAT, USGS, CMA and NOAA.

The main objectives of the Third Lunar Calibration Workshop are to share knowledge and expertise on:

a) The latest dedicated space-based, ground-based and airborne lunar observation campaigns, that can help with refining the current lunar calibration reference.
b) The preparation of lunar irradiance measurements from observations by the instruments to be monitored.
c) Lunar irradiance models and to define a framework for inter-comparing the performances of those models over a common set of geometrical and illumination conditions.
d) Alternative applications of lunar observations for calibration purposes, for instance in the microwave domain, or post-launch assessments, such as geometric and MTF characterization.

This workshop will lead to an updated assessment of the current lunar observation dataset that can either support refining the accuracy of the current version of the ROLO/GIRO or be part of the GSICS Lunar Observation Dataset (GLOD). It will also provide a first assessment of various lunar irradiance models on a common dataset via an inter-comparison exercise. Finally, it is intending to provide more insight on the use of lunar observations in satellite mission Cal/Val plans and for sensor monitoring activities, including in the microwave domain.

A series of preparatory activities is currently being defined for which participants are expected to present their results for discussion at the workshop. A list of topics is available on the GSICS Development Wiki topic dedicated to the 2020 Lunar Calibration Workshop (http://gsics.atmos.umd.edu/bin/view/Development/LunarCalibrationWS2020). Presentations about the latest progress on lunar measurements and Moon observations, using the ROLO/GIRO, inter-calibration using the Moon, applications in the microwaves and alternative usages of lunar imagery are welcome. The workshop aims to trigger activities to enhance the current lunar calibration capabilities, while strengthening further the interactions between the members of the Lunar Calibration Community.

A series of web meetings will be organized, as necessary, in preparation of the workshop. Announcements will be made through the GSICS Developers mailing list. All information and documentation regarding the preparation of the workshop, together with the contact details of the organizers can be found under the GSICS Lunar Calibration wiki topic (http://gsics.atmos.umd.edu/bin/view/Development/LunarWorkArea) or on the 2020 Lunar Calibration Workshop webpage.

GSICS-Related Publications

Alhammoud, B, et al, 2019. "Sentinel-2 Level-1 Radiometry Assessment Using Vicarious Methods From DIMITRI Toolbox and Field Measurements From RadCalNet Database." *Ieee Journal of Selected Topics in Applied Earth Observations and Remote Sensing* 12, no. 9 (September 2019): 3470–79. https://doi.org/10.1109/JSTARS.2019.2936940.

Chang, T and X, Xiong. 'GOES-16/ABI Thermal Emissive Band Assessments Using GEO-LEO-GEO Double Difference'. *Earth and Space Science*, n.d. https://doi.org/10.1029/2019EA000617.

Rodrigo, J.F., J. Gil, P. Salvador, D. Gómez, J. Sanz, and J.L. Casanova. 'Analysis of Spatial and Temporal Variability in Libya-4 with Landsat 8 and Sentinel-2 Data for Optimized Ground Target Location'. *Remote Sensing* 11, no. 24 (2019). https://doi.org/10.3390/rs11242909.

Shrestha, M., N. Hasan, L. Leigh, and D. Helder. "Derivation of Hyperspectral Profile of Extended Pseudo Invariant Calibration Sites (EPICS) for Use in Sensor Calibration." *Remote Sensing* 11, no. 19 (2019). https://doi.org/10.3390/rs11192279.

Return to Page One

doi: 10.25923/ymt5-wz59

Sterckx, S., and E. Wolters. "Radiometric Top-of-Atmosphere Reflectance Consistency Assessment for Landsat 8/OLI, Sentinel-2/MSI, PROBA-V, and DEIMOS-1 over Libya-4 and RadCalNet Calibration Sites." *Remote Sensing* 11, no. 19 (2019). https://doi.org/10.3390/rs11192253.

Zhang, L., P. Zhang, X. Hu, L. Chen, M. Min, N. Xu, and R. Wu. "Radiometric Cross-Calibration for Multiple Sensors with the Moon as an Intermediate Reference." *Journal of Meteorological Research* 33, no. 5 (2019): 925–33. https://doi.org/10.1007/s13351-019-9008-y.

Zeng, Z.-Q., G.-M. Jiang, and Y.-Q. Jin. 'Intercalibration of FY-3C MWRI Brightness Temperature Against GMI Measurements Based on Ocean Microwave Radiative Transfer Model'. In *International Geoscience and Remote Sensing Symposium (IGARSS)*, 8932–35, 2019. https://doi.org/10.1109/IGARSS.2019.8898142.

Submitting Articles to the GSICS Quarterly Newsletter:

The GSICS Quarterly Press Crew is looking for short articles (800 to 900 words with one or two key, simple illustrations), especially related to calibration / validation capabilities and how they have been used to positively impact weather and climate products. Unsolicited articles may be submitted for consideration anytime, and if accepted, will be published in the next available newsletter issue after approval / editing. Please send articles to manik.bali@noaa.gov.

With Help from our friends:

The GSICS Quarterly Editor would like to thank Larry Flynn (NOAA), Tim Hewison (EUMETSAT) and Cheng-Zhi Zou (NOAA) for reviewing articles in this issue.

Published By

GSICS Coordination Center
NOAA/NESDIS/STAR NOAA
Center for Weather and Climate Prediction, C
5830 University Research Court, C2850
College Park, MD 20740, USA

Return to Page One